Radiation Damage in 20-cm Long LYSO:Ce and BaF_2:Y Crystals

Christina Wang, *Member, IEEE*, Liyuan Zhang, Chen Hu, Ren-Yuan Zhu, *Life Senior Member, IEEE*, Kranti Gunthoti, Michael Mocko, Steve Wender, and Zhehui Wang, *Senior Member, IEEE*

***Abstract*— Inorganic scintillators are widely used in high-energy physics (HEP) experiments. Bright and fast cerium-doped lutetium yttrium oxyorthosilicate ($Lu_{2(1-x)}Y_{2x}SiO_5$:Ce or LYSO:Ce or LYSO) crystals are being used to construct the compact muon solenoid (CMS) barrel timing layer (BTL) detector at the high-luminosity large hadron collider (HL-LHC), where up to 2.5-Mrad ionization dose, 1.7×10^{13} charged hadrons/cm^2, and 2×10^{14} n_{eq}/cm^2 are expected. With an ultrafast scintillation of less than 0.6-ns decay time and a suppressed slow component, yttrium-doped barium fluoride (BaF_2:Y) crystal is a promising ultrafast inorganic scintillator for future HEP time of flight and calorimeter applications at the energy and intensity frontiers. The 20-cm-long LYSO:Ce and BaF_2:Y crystals were irradiated by 800-MeV proton beam at the blue room of Los Alamos Neutron Science Center (LANSCE) up to 7.5×10^{15} p/cm^2. We report on the degradation of their optical and scintillation properties.**

***Index Terms*— Barium fluoride, color center, LYSO, proton, radiation damage, scintillators.**

I. Introduction

TOTAL absorption shower counters made of inorganic crystal scintillators have been widely used in high-energy physics (HEP) experiments for decades due to their excellent energy resolution and detection efficiencies [1]. Future HEP experiments at the high-luminosity large hadron collider (HL-LHC), Fermilab, and FCC-hh, however, pose an extreme challenge of severe radiation environment from ionization dose and hadrons. With 3000 fb^{-1} of integrated luminosity, the HL-LHC presents a severe radiation environment, expecting up to 70 (5)-Mrad ionization dose, 3×10^{14} (3×10^{13}) charged hadrons/cm^2, and 3×10^{15} (3×10^{14}) 1-MeV equivalent neutrons/cm^2 for the endcap (barrel) timing detectors [2]. The Mu2e-II experiment expects 0.1–1-Mrad ionization dose on the crystals in the electromagnetic calorimeter [3].

Manuscript received 30 June 2024; revised 15 July 2024; accepted 23 July 2024. Date of publication 29 July 2024; date of current version 18 September 2024. This work was supported in part by U.S. Department of Energy under Grant DE-SC0011925, Grant DE-SC0024094, Grant DE-SC0014664, and Grant DE-AC52-06NA25396. *(Corresponding author: Christina Wang.)*

Christina Wang, Liyuan Zhang, Chen Hu, and Ren-Yuan Zhu are with the Division of Physics, Mathematics and Astronomy, California Institute of Technology, Pasadena, CA 91125 USA (e-mail: christina.wang@caltech.edu; zhu@caltech.edu).

Kranti Gunthoti, Michael Mocko, Steve Wender, and Zhehui Wang are with the Physics Department Los Alamos National Laboratory, Los Alamos, NM 87545 USA.

Color versions of one or more figures in this article are available at https://doi.org/10.1109/TNS.2024.3434441.

Digital Object Identifier 10.1109/TNS.2024.3434441

Bright and fast cerium-doped lutetium yttrium oxyorthosilicate (LYSO:Ce or LYSO) crystals are currently used to construct the compact muon solenoid (CMS) barrel timing layer (BTL) detector for the HL-LHC. LYSO crystals were also proposed to construct total absorption calorimeters for the SuperB experiment in Europe [4] and the Mu2e experiment at Fermilab [5], and a 3-D imaging calorimeter for the HERD experiment in space [6]. However, the high cost of LYSO crystals caused by high Lu_2O_3 price and high melting point limit their use in future large-scale HEP experiments.

With an ultrafast scintillation (0.6 ns) and a suppressed slow component from yttrium doping, yttrium-doped barium fluoride (BaF_2:Y) crystal is a promising ultrafast inorganic scintillator for future time of flight and calorimeter applications. It is currently being considered for a total absorption calorimeter for Phase 2 of the Mu2e experiment at Fermilab [3]. Our early investigation shows that the initial loss of transparency and light output (LO) is stabilized in large size BaF_2 crystals from several vendors against an ionization dose up to 200 Mrad [7]. Follow-on investigations show a similar behavior for mm-thick BaF_2 crystal plates after a proton fluence up to 1×10^{15}/cm^2 [8] and a neutron fluence up to 9×10^{15} n_{eq}/cm^2 [9]. Based on previous study on smaller BaF_2:Y crystal samples [10], this article is our first report on the radiation harness of 20-cm-long BaF_2:Y crystals against gamma rays and protons.

In this article, radiation-induced absorption in 20-cm-long LYSO:Ce and BaF_2:Y samples is measured. Simulation study for the LHC [11] has shown that the expected proton energy spectra are peaked at several hundred MeV, making the 800-MeV proton beam at Los Alamos Neutron Science Center (LANSCE) an ideal tool to investigate charged hadron-induced radiation damage in inorganic scintillators.

We present the result of the proton irradiation experiment 9168 that was conducted in October 2022 at LANSCE with 800-MeV proton beam. The 20-cm-long BaF_2:Y and LYSO:Ce crystal samples were irradiated up to 1.7×10^{13} cm^{-2} and 6.4×10^{15} cm^{-2}, respectively. These crystal samples were also irradiated by Cs-137 γ rays at Caltech, before being irradiated by proton beam. The LYSO:Ce sample was irradiated up to 100 Mrad and the BaF_2:Y samples were irradiated up to 1 Mrad. Their transmittance, radiation-induced absorption coefficient (RIAC), and radiation-induced color center densities are shown for both proton and gamma-ray irradiation.

The rest of this article is organized as follows. Section II describes the experimental setup used for the experiment 9168 at LANSCE. The proton fluence measurement is discussed in Section III; Section IV details the transmittance, RIAC, and color center analysis for BaF_2:Y crystals; Section V reports the LO measurements for BaF_2:Y samples done before proton irradiation; Section VI provides the transmittance and RIAC results for the LYSO:Ce sample; Finally, the summary is presented in Section VII.

II. Proton Irradiation Experiment at LANSCE

The proton irradiation experiment 9168 was conducted in October 2022 at the blue room of the LANSCE using 800-MeV proton beam. The intensity of the beam was adjusted to 5×10^{11} protons per second with a full width at half maximum beam spot of 1 in, covering the entire front surface of the samples.

Optical and scintillation properties of all the crystal samples were characterized at the Caltech Crystal Laboratory before and after irradiation. The variation in crystal transmittance was also measured in situ during and immediately after irradiation. These long crystal samples were wrapped with aluminum foils except the two end faces to allow in situ longitudinal light transmittance measurement. All the samples were placed on a linear stage with their longitudinal axes aligned with the proton beam.

Fig. 1 is a schematic showing the experimental setup used in the experiment 9168, where samples were moved into the proton beam for irradiation and into the measurement position for longitudinal transmittance (LT) data taking in situ [8] through remote control. The entire setup consists of a linear stage, optical fibers, and a lock-in amplifier-based spectrophotometer. The linear stage has a travel distance of 1 m and was used to move the samples into the proton beam or the transmittance measurement position through remote control. Chopped light from a 150-W xenon lamp went through a monochromator, and a small part of the light was monitored by a reference photodiode (Thorlabs DET10A). The majority of the light was injected into the crystal sample via 0.365-mm quartz fibers and through two collimators at the front and back of the sample, and it was measured by a photodiode (Oriel 70336). The lock-in amplifier (Oriel Merlin) measured the ratio between the signal and reference photodetectors. The precision and stability of this ratio is about 1%, and it is free from fluctuations of both the light source intensity and the radiation-induced phosphorescence background in the sample.

Fig. 2 shows a total of eight samples mounted on the linear stage in the experiment 9168. The samples are an LYSO-W Shashlik cell with various wavelength shifter readout, three groups of small LYSO:Ce crystal samples, and LuAG:Ce ceramic samples, denoted as G1, G2, and G3 in the rest of this article, one group of LYSO:Ce crystal bars from various vendors for the CMS BTL detector, a 20-cm-long LYSO:Ce sample from Saint-Gobain, and two 20-cm-long BaF_2:Y samples from Shanghai Institute of Ceramics (SIC) and Beijing Glass Research Institute (BGRI).

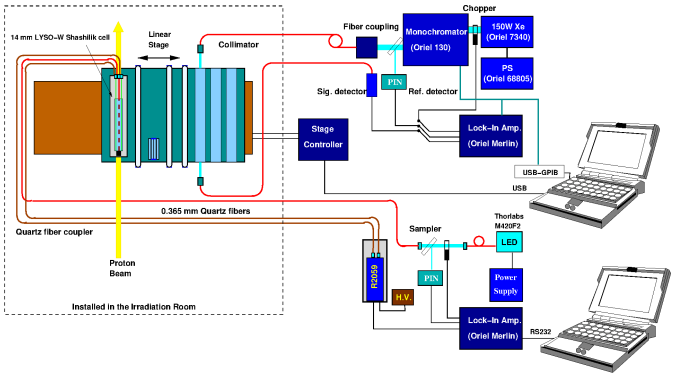

Fig. 1. Schematic showing the setup used to move the crystals into the proton beam and the LT measurement position in situ by remote control during the experiment 9168.

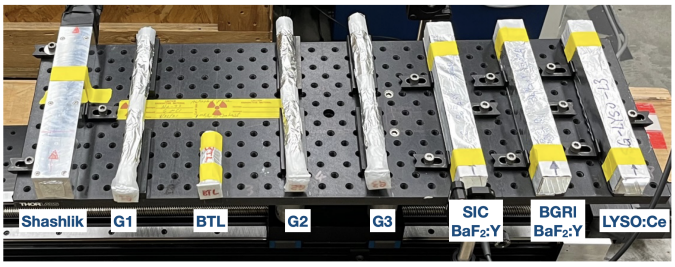

Fig. 2. Photograph showing eight samples mounted on the linear stage. Aluminum foils were taped to the two ends of G1, G2, G3, and BTL crystals and the front face of the Shashlik cell to measure proton fluence.

This article focuses on the LT data measured in situ during the experiment for the 20-cm-long LYSO:Ce and two BaF_2:Y crystal samples. All the irradiated samples were shipped back to Caltech in August 2023 after a ten-month cool down at LANSCE. Their transmittance was also measured at Caltech with a Hitachi U-3210 spectrophotometer with a 0.25% precision, before any irradiation, after γ-ray irradiation, before proton irradiation, and after the ten-month recovery. The transmittance data were used to calculate RIACs and color centers, as described in Sections IV and VI.

The LO of the 20-cm-long BaF_2:Y samples measured before and after several integrated doses of γ irradiation is presented in Section V. The LO was measured by a Hamamatsu R2059 photomultiplier tube (PMT) with a grease coupling to the sample excited by 0.511-MeV γs from a Na-22 source with a coincidence trigger. The systematic uncertainty of the LO measurement is about 1%.

III. Proton Fluence Measurement With Activated Aluminum Foil

To accurately measure the proton fluence, we measured the activation of Al foils that are taped to the two ends of some of the crystal samples during proton irradiation, which is a standard technique for proton fluence measurement used by the CERN proton irradiation facility and the Fermilab irradiation test area. Compared with the fluence from integrating beam current data, the fluence obtained by measuring activated Al foil takes into account the additional variations in the beam shape, beam shaking, and misalignment. Therefore, a correction factor is derived from comparing the proton

fluence calculated from Al foils with that from the beam current for a subset of samples that had Al foils taped. The correction factor is then applied to the fluence calculated from the beam current data for all the samples. The integrated proton fluence was determined by measuring the number of Na-22 photons in the aluminum foils activated by protons as

$$F = \frac{N_i}{N_a \times \sigma} \tag{1}$$

where N_i is the number of Na-22 atoms produced in aluminum foil by proton activation, N_a is the total number of aluminum atoms in the foil determined by measuring the aluminum foil mass, and σ is the proton activation cross section of Na-22 in aluminum, which is 15.42 ± 0.56 mb for 800-MeV proton [12].

N_i is calculated from the radioactivity of Na-22

$$N_i = \frac{dN}{dt} \times e^{t/\tau} \times \tau \tag{2}$$

where (dN/dt) is the measured radioactivity, t is the time elapsed between the irradiation and Na-22 radioactivity measurement, and τ is the lifetime of Na-22, which can be obtained from the half-life of Na-22 ($t_{1/2} = \tau \ln 2$), which is 950.8 ± 0.9 days. The radioactivity measurement of Na-22 is described in Section III-A.

During the proton irradiation experiment, the aluminum foils were taped to the two ends of four groups of samples: G1, G2, G3, and BTL samples, as well as the front of the Shashlik cell to measure the proton fluence. Aluminum foils were not taped to the back of the Shashlik cell and the two ends of the 20-cm-long BaF_2:Y and LYSO:Ce samples, where optical cables and light from optical fibers were used to readout the sample response in situ. The proton fluence calculated from Al foils are compared with the time integration of the LANSCE beam current data and used to calculate a correction factor for the proton fluence calculated from beam current data for all the samples.

A. Na-22 Radioactivity Measurement

We measured the rate of 1.27-MeV gamma rays from the activated Al foils with a high-purity germanium detector (Ortec GEM30P) at Caltech 350 days after proton irradiation. The measured rate was then used to calculate the corresponding radioactivity of Na-22 using a calibrated 1.5-μCi Na-22 source with an uncertainty of 3%. Both the Al foil samples and the calibration source were measured with the same geometrical configuration with a detection solid angle of about 0.075 sr and dead time of <1%. The proton fluence was then determined by the measured radioactivity of Na-22 and (1) and (2). The uncertainty of the proton fluence is 4.4%, dominated by a 3.6% systematic uncertainty on the proton-induced activation cross section and 2%–12% statistical uncertainty from the Na-22 peak measurement.

Table I shows the proton fluence data for the five Al foils placed at the front of the samples. The proton fluence measured from Al foil A is 60% larger, due to scattering and proton shower leakage from the adjacent Shashlik cell irradiated up to 5×10^{15} p/cm^2. To reduce this scattering and shower background, we calculate the correction factor for the proton fluence using only the Al foils from samples with the higher fluence compared with its neighboring samples, i.e., Al foils C and E. The correction factor is calculated to be 0.86 ± 0.15 and is applied to all the proton fluences calculated using the beam current data provided by LANSCE.

TABLE I
PROTON FLUENCE MEASUREMENT FOR THE FRONT Al FOILS

Al foil label Al foil crystals	A G1	B G2	C G3	D BTL	E Shashlik
Fluence from beam current [cm^{-2}]	1.2E+13	3.7E+14	2.2E+15	2.8E+13	5.4E+15
Fluence from Al foil [cm^{-2}]	1.9E+13	3.0E+14	1.8E+15	2.7E+13	4.9E+15
Uncertainty from Al foil [cm^{-2}]	2.3E+12	1.7E+13	8.5E+13	2.5E+12	2.3E+14
Relative uncertainty	13%	6%	5%	10%	5%
Ratio between two measurements	1.56	0.80	0.81	0.95	0.92

TABLE II
PROTON FLUENCE MEASUREMENT FOR THE BACK Al FOILS

Al foil label Al foil crystals	G G1	H G2	I G3	F BTL
Fluence from beam current [cm^{-2}]	1.2E+13	3.7E+14	2.2E+15	2.8E+13
Fluence from Al foil [cm^{-2}]	4.0E+13	1.7E+14	8.5E+14	2.3E+13
Uncertainty from Al foil [cm^{-2}]	3.9E+12	1.2E+13	4.5E+13	2.4E+12
Relative uncertainty	10%	7%	5%	10%
Ratio between two measurements	3.35	0.47	0.39	0.83

Table II shows the proton fluence data from the four Al foils placed at the back of samples. For the crystals that have Al foils on both the ends, the back-to-front foil fluence ratio is 2.15 ± 0.34, 0.59 ± 0.05, 0.48 ± 0.03, and 0.87 ± 0.12, for G1, G2, G3, and BTL, respectively.

The proton fluence measured from the Al foil G is three times larger because of the scattering and shower from the adjacent Shashlik cell that was irradiated up to 5×10^{15} p/cm^2. For sample G3, which is the sample that is least affected by the background effect from adjacent samples, the back-to-front foil fluence ratio is 48%, which is consistent with the multiple scattering effect of 800-MeV protons in LYSO:Ce crystals [13].

In a brief summary, the proton fluence measured using the activated Al foils is consistent with the LANSCE beam current data. The correction factor of 0.86 ± 0.15 was determined using the highest fluence foils C and E and was applied to all the proton fluence values obtained from the beam current integration. The observed back-to-front ratio of 48% is consistent with the expected multiple scattering effect of 800-MeV protons in LYSO:Ce crystals.

IV. LT, RIAC, AND COLOR CENTERS IN BaF_2:Y

Fig. 3 shows the transmittance history for two BaF_2:Y samples from BGRI (top) and SIC (bottom). Also shown in the figures are the x-ray excited luminescence spectra (dots) and the numerical values of the emission-weighted LT (EWLT) for

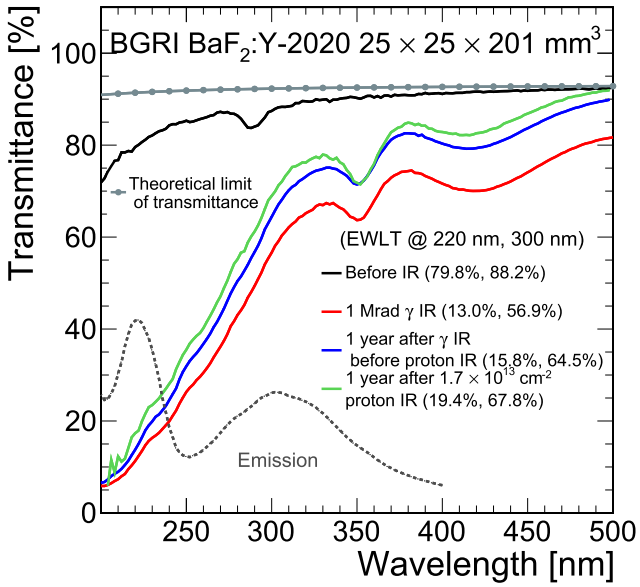

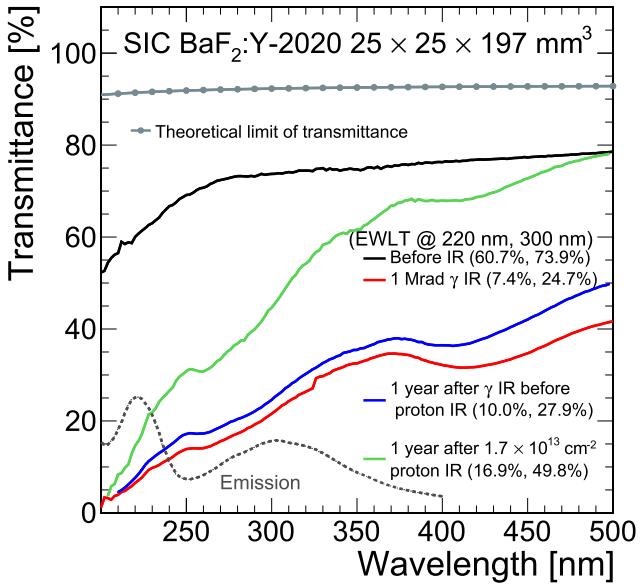

Fig. 3. LT history is shown for two 20-cm-long BaF_2:Y samples before irradiation (black), after 1-Mrad γs (red, 2021), one year after γ irradiation just before proton irradiation (blue, 2022) and one year after by 1.7×10^{13} cm^{-2} proton irradiation (green, 2023), showing damage recovery after 1-Mrad ionization and after 1.7×10^{13} p/cm^2.

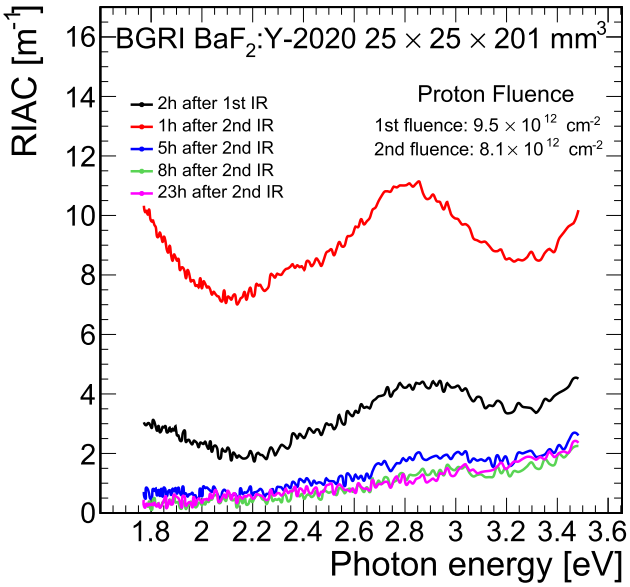

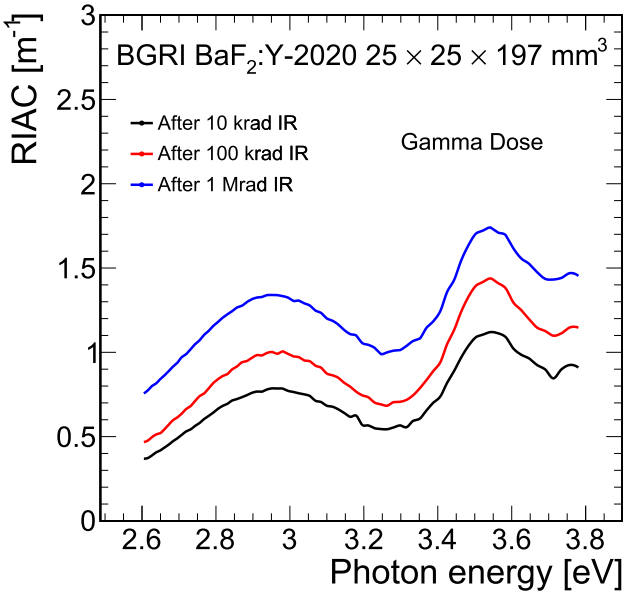

Fig. 4. Proton-induced (top) and gamma-induced (bottom) absorption coefficient are shown for the BGRI BaF_2:Y sample. To reduce statistical uncertainty, only data points with LT > 5% are shown in the figures.

the BaF_2:Y fast and slow components, integrated from 200 to 250 nm and 250 to 400 nm, respectively. The EWLT is defined as

$$\mathrm{EWLT} = \frac{\int \mathrm{LT}(\lambda)\mathrm{Em}(\lambda)d\lambda}{\int \mathrm{Em}(\lambda)d\lambda} \tag{3}$$

where LT is the longitudinal transmittance and $\mathrm{Em}(\lambda)$ is the x-ray exited emission spectrum. Both the samples were irradiated first by 1 Mrad of γ rays in 2021 and by 1.7×10^{13} cm^{-2} of proton irradiation in 2022 at LANSCE. The EWLT data show a long-term recovery a year after the 1-Mrad ionization and a year after the 1.7×10^{13} p/cm^2 irradiation in both BaF_2:Y samples.

We calculate the light attenuation length (LAL) as a function of wavelength [1] using the LT data

$$\mathrm{LAL}(\lambda) = \frac{l \times \left[\sqrt{4T_s^4(\lambda) + T^2(\lambda)(1 - T_s^2(\lambda))^2} - 2T_s^2(\lambda)\right]}{\ln\left[T(\lambda)\left(1 - T_s^2(\lambda)^2\right]\right.} \tag{4}$$

where $T(\lambda)$ is the LT measured along crystal length l, and $T_s(\lambda)$ is the theoretical transmittance assuming multiple bounces between the two ends of the crystal and without internal absorption

$$T_s(\lambda) = \frac{1 - R(\lambda)}{1 + R(\lambda)} \tag{5}$$

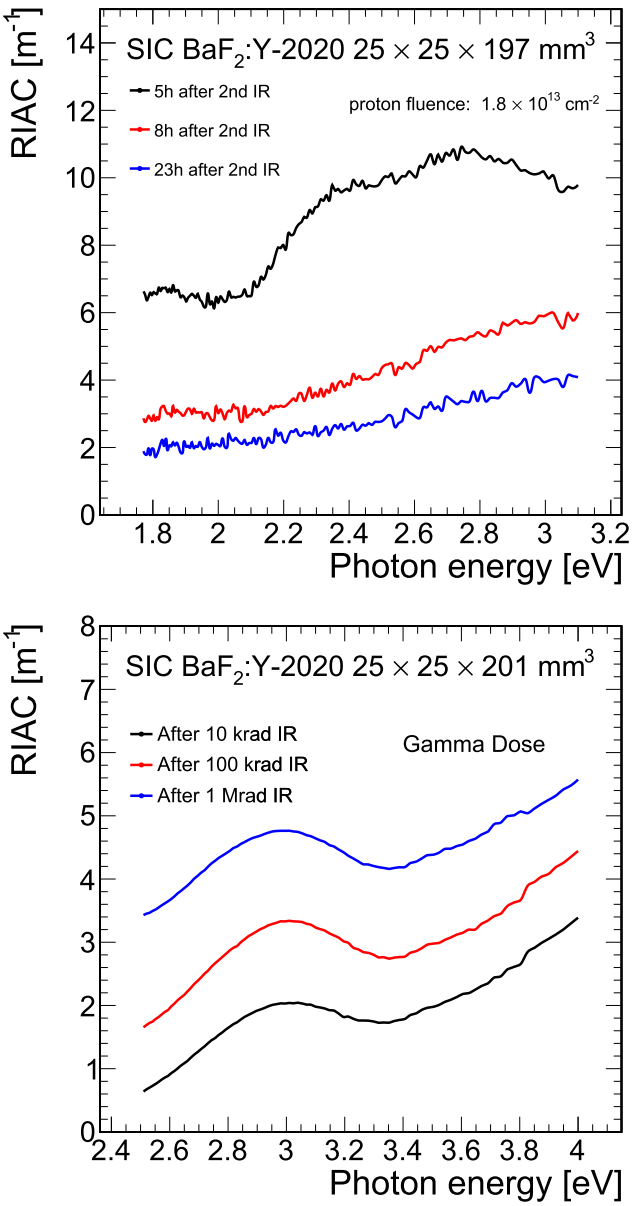

Fig. 5. Proton-induced (top) and gamma-induced (bottom) absorption coefficient are shown for the SIC BaF_2:Y sample. To reduce statistical uncertainty, only data points with LT > 5% are shown in the figures.

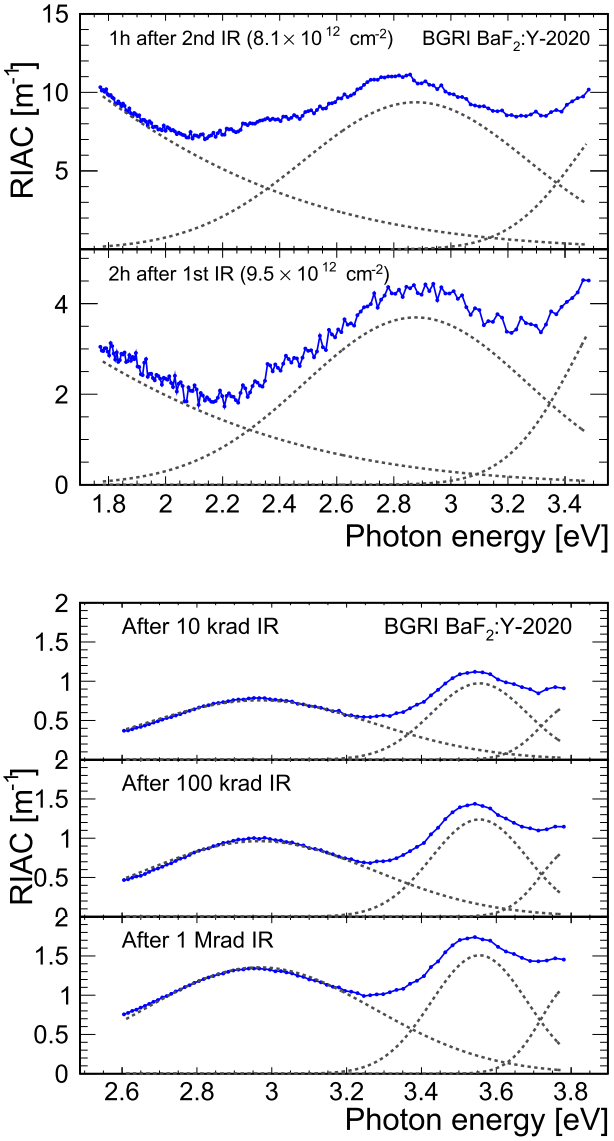

Fig. 6. Proton (top) and gamma (bottom)-induced absorption coefficients are shown for the BGRI BaF_2:Y sample.

and

$$R(\lambda) = \frac{(n_{\text{crystal}}(\lambda) - n_{\text{air}}(\lambda))^2}{(n_{\text{crystal}}(\lambda) + n_{\text{air}}(\lambda))^2} \tag{6}$$

where $n_{\text{crystal}}(\lambda)$ and $n_{\text{air}}(\lambda)$ are the refractive indices for crystal and air, respectively.

By comparing the LAL of a crystal before and after irradiation, the RIAC or the color center density and the emission weighted RIAC (EWRIAC) can be calculated [1]

$$\text{RIAC}(\lambda) \text{ or } \text{D}(\lambda) = 1/\text{LAL}_{\text{after}}(\lambda) - 1/\text{LAL}_{\text{before}}(\lambda) \tag{7}$$

$$\text{EWRIAC} = \frac{\int \text{RIAC}(\lambda)\text{Em}(\lambda)d\lambda}{\int \text{Em}(\lambda)d\lambda} \tag{8}$$

where $\text{LAL}_{\text{before}}(\lambda)$ and $\text{LAL}_{\text{after}}(\lambda)$ are the LAL before and after irradiation, respectively, and $\text{Em}(\lambda)$ is the emission spectrum.

Figs. 4 and 5 show the RIAC spectra calculated using the above equations for the BaF_2:Y samples from BGRI and SIC, respectively. The LT measured in situ during the proton irradiation experiment at LANSCE was only measured down to 350 nm, translating to an RIAC data available up to 3.5 eV. We note short-term recovery in a few hours during proton irradiation in both the samples, which may be attributed to thermal relaxation.

The RIAC spectrum can be decomposed to a sum of several color centers with Gaussian energy distributions [1]. The results of the fit for the proton-induced absorption coefficients (top) and the gamma-induced absorption coefficients (bottom) are shown in Figs. 6 and 7 for the BGRI and SIC BaF_2:Y samples, respectively. Both proton and gamma-induced

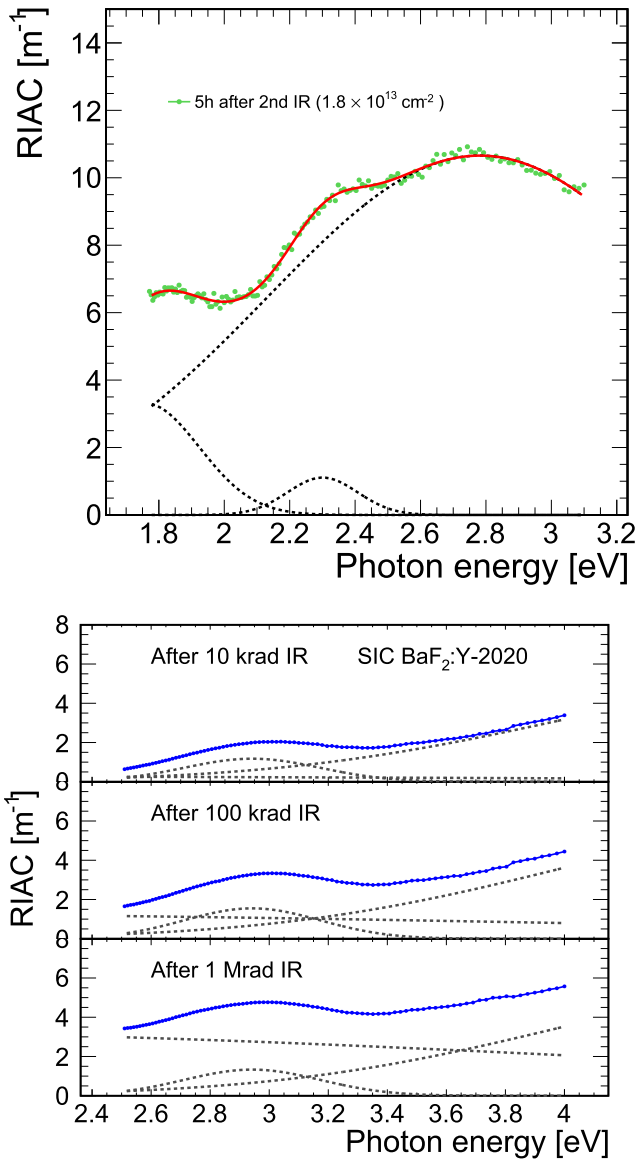

Fig. 7. Proton (top) and gamma (bottom)-induced absorption coefficients are shown for the SIC BaF_2:Y sample.

TABLE III

GAMMA (a) AND PROTON-INDUCED (b) COLOR CENTERS EXTRACTED FOR THE BGRI BaF_2:Y SAMPLE, WHERE E, A, AND σ ARE THE ENERGY, WIDTH, AND AMPLITUDE, RESPECTIVELY, USED IN THE FITS

(a)

E/σ [eV]	A (10 krad) [m^{-1}]	A (100 krad) [m^{-1}]	A (1 Mrad) [m^{-1}]
3.0/0.3	0.8	1.0	1.4
3.6/0.1	1.0	1.2	1.5
3.8/0.1	0.7	0.9	1.2

(b)

E/σ [eV]	A (2h) [m^{-1}]	A (1h) [m^{-1}]
1.2/1.1	4.9	10.0
2.9/0.4	3.7	9.4
3.7/0.2	9.2	33

absorption coefficients can be described by three color centers of Gaussian energy distributions.

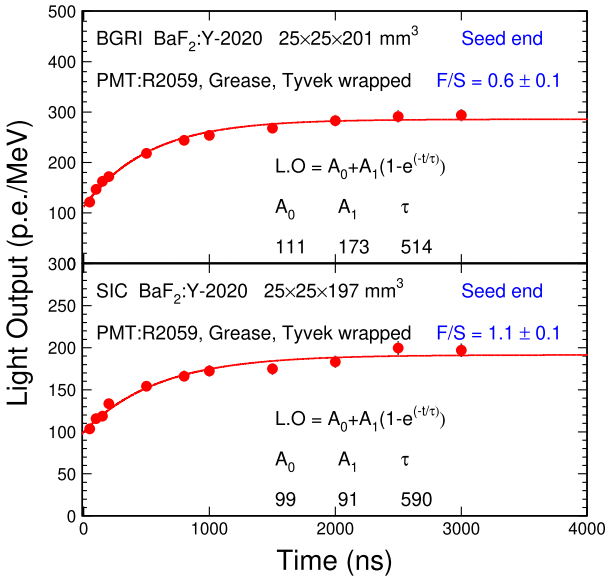

Fig. 8. LO is shown as a function of the integration time for the BGRI (top) and SIC (bottom) BaF_2:Y samples with their seed end coupled to the PMT.

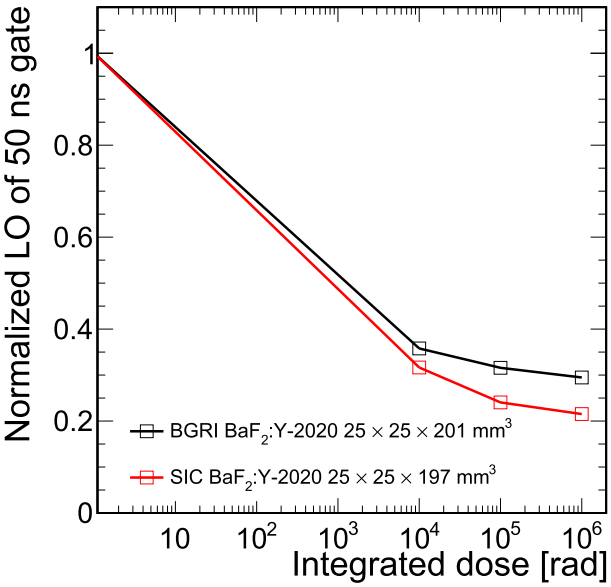

Fig. 9. Normalized LO integrated in 50-ns gate is shown as a function of integrated dose. All the LO values are normalized to that measured before irradiation.

Tables III and IV list the fit results of the energy, amplitude, and width of the color centers for the BGRI and SIC BaF_2:Y samples, respectively. For the BGRI BaF_2:Y sample, the proton-induced color centers have photon energy of 1.2, 2.9, and 3.7 eV, while the gamma-induced color centers are at 3, 3.6, and 3.8 eV. Two of the proton-induced color centers are slightly shifted from the gamma-induced color centers. For the BGRI BaF_2:Y sample, the proton-induced color centers have photon energy of 1.8, 2.3, and 2.8 eV, while the gamma-induced color centers are at 1.5, 2.9, and 4.9 eV. A combined fit to the proton- and gamma-induced absorption coefficients by constraining the two proton- and gamma-induced color centers to have the same photon energy did not converge,

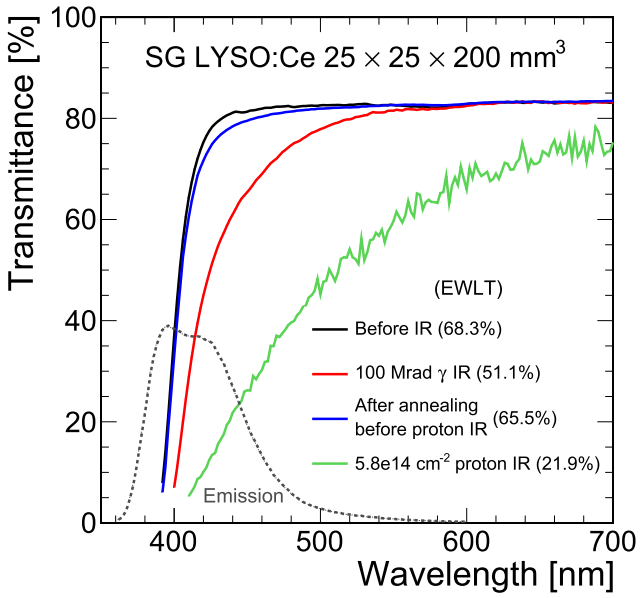

Fig. 10. LT history is shown for the 20-cm-long LYSO:Ce sample before irradiation (black, 2015), after 100 Mrad (red, 2015), after thermal annealing before proton irradiation (blue, 2022), and one year after 5.8 × 10^{14} cm^{-2} of proton fluence (green, 2023).

TABLE IV

GAMMA (a) AND PROTON-INDUCED (b) COLOR CENTERS EXTRACTED FOR THE SIC BaF_2:Y SAMPLE, WHERE E, A, AND σ ARE THE ENERGY, WIDTH, AND AMPLITUDE, RESPECTIVELY, USED IN THE FITS

(a)

E/σ [eV]	A (10 krad) [m^{-1}]	A (100 krad) [m^{-1}]	A (1 Mrad) [m^{-1}]
1.5/2.6	0.3	1.2	3.2
2.9/0.2	1.2	1.6	1.3
4.9/4.0	5.1	5.8	5.7

(b)

E/σ [eV]	A (5h) [m^{-1}]
1.8/0.2	1.4
2.3/0.1	0.3
2.8/0.7	17.3

indicating that the proton- and gamma-induced color centers are distinct from each other.

V. LO FOR BaF_2:Y

The LO before and after irradiation was measured by a Hamamatsu R2059 PMT with a grease coupling to the sample excited by 0.511-MeV γs from a Na-22 source with a coincidence trigger for the BaF_2:Y samples. The samples were wrapped with Tyvek paper to improve light collection efficiency. The systematic uncertainty of LO measurement is about 1%. Fig. 8 shows the integrated LO as a function of the integration time for 0.511-MeV photons and the corresponding fit with a sum of a constant and an exponential function. The ratio between the constant and the amplitude of the exponential function represents the ratio between the fast and slow scintillation light (F/S) and is calculated to be 0.6 ± 0.1 and 1.1 ± 0.1 for the BGRI and SIC BaF_2:Y samples, respectively. In addition, the time constants of the slow decay component are extracted as 514 and 590 ns for the BGRI and SIC BaF_2:Y samples, respectively.

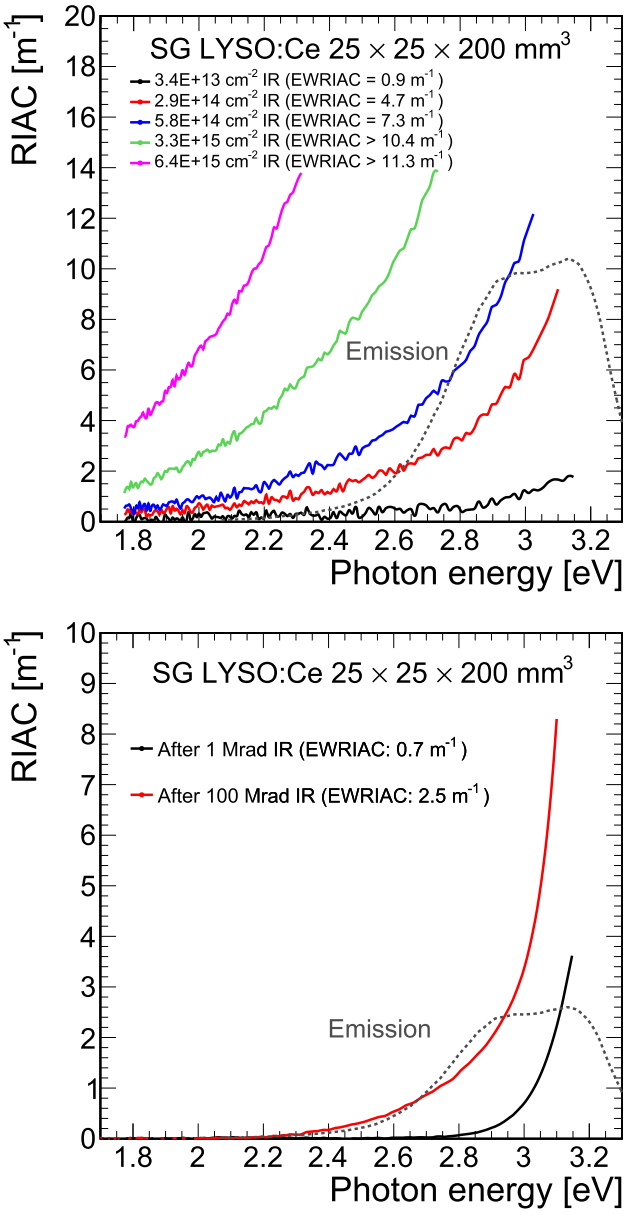

Fig. 11. Proton-induced (top) and gamma-induced (bottom) absorption coefficient are shown for the LYSO:Ce sample. To ensure enough statistics, only data points with LT > 5% are shown.

Fig. 9 shows the normalized LO in 50 ns after γ-ray irradiation of 10, 100 krad, and 1 Mrad for the BGRI (top) and SIC (bottom) BaF_2:Y samples. While the saturated damage is more or less maintained, the LO is degraded to 20%–30% of that before irradiation, indicating that yttrium doping may affect negatively to radiation hardness in BaF_2 crystals.

VI. LT AND RIAC FOR LYSO:CE

The LYSO:Ce sample was irradiated first by 100 Mrad of γ rays in 2015, followed by a thermal annealing and then by 5.8 × 10^{14} cm^{-2} of proton irradiation in 2022 at LANSCE. Fig. 10 shows the LT history for the LYSO:Ce sample, confirming previous measurements [7], [8], [14] and simulation [15] that showed good LT and low EWRIAC values

after both gamma dose and proton fluence well beyond that expected at the HL-LHC.

Fig. 11 shows the proton- and gamma-induced absorption coefficients. This LYSO:Ce sample demonstrates EWRIAC values of 2.5 m^{-1} after 100 Mrad and 0.9 m^{-1} after 3.4×10^{13} p/cm^2, exceeding the CMS BTL specification: <3 m^{-1} after 2.5 Mrad and 1.7×10^{13} p/cm^2. In addition, no color centers were identified in both proton- and gamma-induced absorption coefficient distributions.

VII. Conclusion

Two 20-cm-long BaF_2:Y samples were irradiated up to 1 Mrad and 1.7×10^{13} p/cm^2. Fast recovery was observed in several hours after proton irradiation, which may be partly attributed to thermal relaxation observed in our previous investigations. Radiation-induced color centers in BaF_2:Y samples were analyzed with distinct color centers for proton and gamma irradiation with photon energy between 1 and 4 eV. We observed different color centers between proton and gamma irradiation. BaF_2:Y samples from two vendors also show different color center and recovery patterns, which may be due to different impurities in the raw materials. R&D is ongoing to continue developing BaF_2:Y for its future applications in high rate experiments, such as the Mu2e-II experiment at Fermilab.

The 20-cm-long LYSO:Ce sample shows excellent radiation hardness against γ-rays up to 100 Mrad and protons up to 6.4×10^{15} p/cm^2 with no color centers identified. The data confirm that LYSO:Ce is a promising material for a severe radiation environment expected by future HEP experiments at the energy frontier, such as that at the HL-LHC and the proposed FCC-hh.

References

[1] R.-Y. Zhu, *Radiation Damage Effects*. Cham, Switzerland: Springer, 2020, pp. 1–25, doi: 10.1007/978-3-319-47999-6_22-2.

[2] (Sep. 2019). *A MIP Timing Detector for the CMS Phase-2 Upgrade*. CERN. [Online]. Available: https://cds.cern.ch/record/2667167

[3] K. Byrum et al., "Mu2e-II: Muon to electron conversion with PIP-II," in *Proc. Snowmass*, Mar.2022, pp. 1–46.

[4] G. Eigen et al., "A LYSO calorimeter for the SuperB factory," *Nucl. Instrum. Methods Phys. Res. Sect. A, Accel., Spectrometers, Detect. Associated Equip.*, vol. 718, pp. 107–109, Aug. 2013. [Online]. Available: https://www.sciencedirect.com/science/article/pii/S0168900212014477

[5] G. Pezzullo et al., "The LYSO crystal calorimeter for the Mu2e experiment," *J. Instrum.*, vol. 9, no. 3, Mar. 2014, Art. no. C03018, doi: 10.1088/1748-0221/9/03/c03018.

[6] M. Xu, "The high energy cosmic radiation facility onboard China's space station," *Nucl. Part. Phys. Proc.*, vols. 279–281, pp. 161–165, Oct. 2016. [Online]. Available: https://www.sciencedirect.com/science/article/pii/S2405601416302048

[7] F. Yang, L. Zhang, and R.-Y. Zhu, "Gamma-ray induced radiation damage up to 340 mrad in various scintillation crystals," *IEEE Trans. Nucl. Sci.*, vol. 63, no. 2, pp. 612–619, Apr. 2016.

[8] C. Hu et al., "Proton-induced radiation damage in BaF_2, LYSO, and PWO crystal scintillators," *IEEE Trans. Nucl. Sci.*, vol. 65, no. 4, pp. 1018–1024, Apr. 2018.

[9] C. Hu et al., "Neutron-induced radiation damage in LYSO, BaF_2, and PWO crystals," *IEEE Trans. Nucl. Sci.*, vol. 67, no. 6, pp. 1086–1092, Jun. 2020.

[10] C. Hu, C. Xu, L. Zhang, Q. Zhang, and R.-Y. Zhu, "Development of yttrium-doped BaF_2 crystals for future HEP experiments," *IEEE Trans. Nucl. Sci.*, vol. 66, no. 7, pp. 1854–1860, Jul. 2019.

[11] *The CMS Electromagnetic Calorimeter Project: Technical Design Report*, Technical Design Report, CMS, CERN, Geneva, Switzerland, 1997. [Online]. Available: https://cds.cern.ch/record/349375

[12] H. Matsuda, S. Meigo, and H. Iwamoto, "Proton-induced activation cross section measurement for aluminum with proton energy range from 0.4 to 3 GeV at J-PARC," *J. Nucl. Sci. Technol.*, vol. 55, no. 8, pp. 955–961, Aug. 2018, doi: 10.1080/00223131.2018.1461694.

[13] K. Nakamura, "Review of particle physics," *J. Phys. G, Nucl. Part. Phys.*, vol. 37, no. 7, Jul. 2010, Art. no. 075021.

[14] G. Dissertori et al., "Results on damage induced by high-energy protons in LYSO calorimeter crystals," *Nucl. Instrum. Methods Phys. Res. A, Accel. Spectrom. Detect. Assoc. Equip.*, vol. 745, pp. 1–6, May 2014. [Online]. Available: https://www.sciencedirect.com/science/article/pii/S0168900214001399

[15] G. Dissertori, C. M. Perez, and F. Nessi-Tedaldi, "A FLUKA study towards predicting hadron-specific damage due to high-energy hadrons in inorganic crystals for calorimetry," *J. Instrum.*, vol. 15, no. 6, Jun. 2020, Art. no. P06006, doi: 10.1088/1748-0221/15/06/p06006.